Effect of Filler Distribution and Caliper Variations on Toner Transfer in Electrophotographic Printing

Nikolas Provatas, Andrew Cassidy** and Mitsuo Inoue****
**McMaster University, Hamilton, Ontario, Canada*
***McGill University, Montreal, Quebec, Canada*
**** PAPRICAN, Pointe Claire, Quebec, Canada*

Abstract

Print density mottle in solid black electrophotographic printing was shown in a previous report to be strongly linked to the distribution of PCC fillers in paper. A model of toner transfer showed qualitatively that toner transfer efficiency is locally increased in regions of high filler density. In this report we extend the previous work by quantifying effect of filler distribution and of paper calliper variations on toner transfer in electrophotography. We modeled the complete electrostatic force field structure within a paper-air-toner transfer gap during electrophotography. By relating effective local dielectric constant to filler concentration, we computed the difference effects that surface and bulk PCC fillers have on the local toner transfer force field. The toner transfer force was found to be higher when the PCC filler was distributed homogeneously throughout the bulk thickness rather than localized at the surface of the paper. Quantitative model of in-plane variations in toner transfer force as a function of corresponding in-plane variations of the effective paper dielectric showed that the variation in paper dielectric on the scale of 500μm or larger contribute significantly to toner transfer force variations. We also found that the higher filler content amplified the effect of caliper non-uniformities on the toner transfer force variations.

Introduction

Recent advances in the science of electrophotography have made Xerographic printing[1-3] a commercially viable alternative to conventional printing in the area of short-run and production colour printing. One of the crucial requirements for high quality printing in Xerography lies in the production of uniform solid prints. Since toner penetrates very little into the paper, even after thermal fusing, print density mottle or toner thickness variation is primarily the result of uneven toner transfer onto the paper surface. This can be caused by a variety of sources, such as spatial variations in surface roughness, paper thickness, moisture and, as has been shown more recently, filler concentration.[4]

Electrophotographic printing relies on *electrostatic* transfer of toner from a photoreceptor plate onto the paper surface under an *electric field*. In the past, paper has often been treated as a uniform layer in designing the electrophotographic printing processes.[1-3] In practice, paper is quite non-uniform, leading to many printing-performance problems in electrophotography.[5] In the specific case of print density mottle, Reference [4] showed that print density mottle in copy-grade paper exhibited strong non-uniformity on scales of ~1mm, a feature size that was also found in filler distribution power spectra. Computational modeling of toner transfer[4] onto simulated paper structures[6] showed, qualitatively, that the higher dielectric constant of PCC filler (known to create a higher overall *average* paper dielectric[7,8]) increases the *local* toner transfer forces, promoting more toner transfer in filler-rich regions of paper.

In this report we extend the modeling work[4] in order to *quantify* toner transfer efficiency as a function of specific paper structures. We begin with a *complete* description of electrostatic transfer forces-field structure within an electrophotographic transfer nip. The new model is described in Section 1 is based on Maxwell's equations of electrostatics, coupled to a spatially varying *dielectric field*. This dielectric field can describe the general non-uniformity of any paper structure in the transfer gap. It can be derived from either simulated paper structures[6] or micrographs of paper samples. (Details of the model and some approximate solutions are given in Appendix A). In Section 2, the model is used to compute the relationship between toner transfer force and filler concentration for near-surface or through-the-bulk deposits. In Section 3, we quantify how the in-plane variations of toner transfer is affected as a function of in-plane variations of the effective paper dielectric. Finally, Section 4 discusses the effect of in-plane variations of local paper thickness on local toner transfer force.

1. Modeling The Electrostatics of Toner Transfer

In most literature describing electrophotography, the main emphasis is placed on the electrostatics of the photoreceptor plate, and the development of latent images.[1-3]

The paper is usually treated as a homogeneous uniform material whose main contribution to the electrostatics of toner transfer enters through its dielectric constant. A uniform toner charge density - σ_t is given on the surface of a photoreceptor. It is originally adhered there by an "adhesion image charge" of opposite sign. Positive charges (the charge density σ_f) are deposited on the top surface of the paper by corona discharge. This charge density establishes an electric field (potential, V) with respect the photoreceptor at the bottom of the figure. This field draws toner (represented here as a charge layer of surface density σ_t) to the paper when the paper passes the transfer region and is "peeled" away from the photoreceptor.

In real paper, non-uniformity in the local dielectric constant and paper caliper will lead to spatial variations in the local electric field in the small transfer region between the photoreceptor and the paper. This is illustrated schematically in Fig. 1, which shows a cross-section of paper-air-toner transfer gap. The cross section is divided into local cells as denoted by index j = 1,2….. Each cell exhibits an average corona charge $< \sigma_f >_j$ and a z-direction electric field $< E_z >_j$. (Brackets denote the average over the cross-section of each cell.) Variations of these quantities from cell reflect the general heterogeneity of paper structure (fibre, filler, paper caliper, moisture, etc).

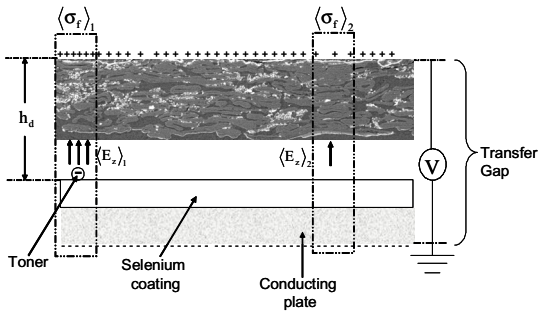

Figure 1. Illustration of spatial variations in toner transfer forces in the case of real paper. Paper heterogeneity causes non-uniformity in the dielectric constant and, as a result, in the electric fields in the toner transfer nip.

To obtain realistic *point-to-point* variation of the electrostatic transfer field, $\vec{E}(\vec{x})$, we solve the fundamental equations of electrostatics throughout the transfer gap. The domain in which these equations are solved – the transfer gap – comprises a "sandwich" of paper, air gap, toner layer and photoreceptor, maintained at a voltage V (see Fig. 1). Since the emphasis of this report is on the role of *paper structures* on electrophotography, we model the photoreceptor as a simple conducting plate. We further assume the voltage in the transfer gap is DC, and neglect the conductivity of the paper due to salts and moisture. This important issue will be incorporated in upcoming reports.

Solving the continuum equations of electrostatics has two main advantages. First, we can model a *general* toner charge distribution $\rho(\vec{x})$. In this report the toner layer is 10 µm thick, with charge density of about 24 C/m^3 (obtained by dividing the charge typical of a 10 µm diameter toner, 1 x 10^{-14} C, by its volume). The second and *most fundamental aspect* of the model is the use of a general dielectric function $\varepsilon(\vec{x})$ at the deposition $\vec{x}$ = (x, y, z) within the transfer region. It is through this function that we can model the effects of paper structure. In this report, paper was taken to comprise three materials, cellulose (main component of fibres), air (pores), and PCC (filler). Their dielectric constants were taken as 3, 1 and 9, respectively. The dielectric of toner was assumed to be 5.

Numerical computations were done in 2D using the finite–elment method. Analytical solutions are applicable to general three-dimensional paper structures. Numerical calculations were performed on the new 10-node Linux-based ("beowolf") PC-Cluster at Paprican. Figure 2 shows the typical structure of the electrostatic field in paper cross section inserted between two conducting plates held at a voltage V, as determined from our toner transfer model. Figure 2(a) shows a colour-coded dielectric map, digitized directly from a micrograph of a paper cross section. Figures 2(b) and 2(c) show the z and x-direction electric fields throughout the gap. We observed that toner transfer force variations in the z-direction across the paper surface depend on the PCC filler content and paper thickness variations within the cell. Generally, higher toner transfer forces were found in the region where higher PCC content and/or higher thickness of the paper. Electrostatic force variations in the lateral direction, although smaller than the z-directional force variations, depend on the distribution of the PCC filler near the paper surface. This lateral force contributes to the scattering of toner depositions, and thus image definition.

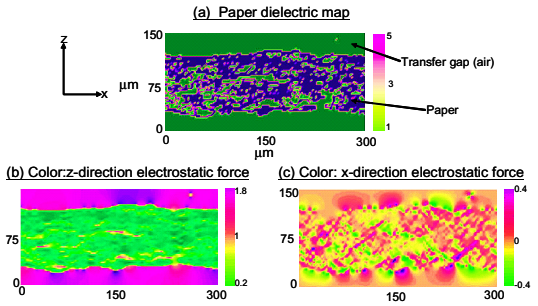

Figure 2. Simulated electrostatic fields within paper and the transfer gap. Fig. 2(a) shows a digitized dielectric map from a SEM micrograph of a cross-section of paper. Green colour represents air and dark blue fibres. Figure 2(b) and 2(c) show the z-and x components of the electric field, respectively. Units are dimensionless.

2. Effects of Filler Distribution Through the Thickness on the Toner Transfer Forces

PCC filler has been shown to play a leading role in controlling the non-uniformity of paper dielectric and, hence, toner transfer force.[4] The reason is that regions with higher

PCC concentrations generally produce a higher local dielectric. This has also been confirmed experimentally with respect to the over all dielectric of paper.[7] (We note that filler can also affect local moisture content, which will further affect the local dielectric. This filler-induced effect of moisture will be explained in a future report.) Remaining questions are to what degree the z-directional PCC distributions affect local toner transfer force and how these can be related to an effective dielectric of filled paper. To isolate and quantify the role of filler specifically, we examine two types of filler distributions within paper. The first is a thin layer of filler concentrated on the top paper surface. The second is a uniform filler distribution throughout the bulk of paper. In both configurations, the concentration of filler was varied, and the strength of the corresponding electrostatic transfer force was computed. To elucidate only the role of filler heterogeneity, non-filler portions of paper were treated as a continuum of cellulose.

Figures 3(a) and 3(b) show two configurations of the filler distributions in the paper. The fibre network represented in light grey and the filler represented by white pixels. Fig. 3(a) shows filler randomly distributed in a layer near the surface within thickness of 30μm, with a concentration, while Fig. 3(b) shows same amount of filler distributed throughout the bulk of paper of 100μm.

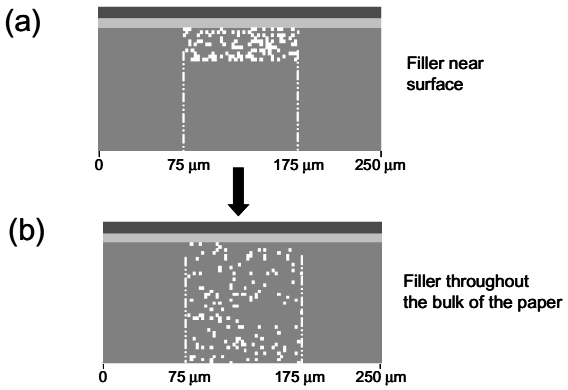

Figure 3. Two types of filler distributions examined. In (a) filler is distributed near the surface. In (b) it extends throughout the bulk.

To calculate toner transfer force over the filled section of paper, we developed another model, in addition to the continuous model. The toner transfer gap was modeled as a triple-layer dielectric system consisting of air gap, filled layer and unfilled layer, as shown in Fig. 4(a). The force per unit charge (i.e., the electric field) in the air gap is:

$$F_z = \frac{-q_T\left[V - \dfrac{\rho\left(h_g - h_T\right)^2}{2\varepsilon_o\varepsilon_T}\right]}{\left[\dfrac{h_c}{\varepsilon_c} + \dfrac{\left(h_p - h_c\right)}{\varepsilon_f} + \dfrac{\left(h_g - h_T\right)}{\varepsilon_T} + \dfrac{\left(h_T - h_p\right)}{\varepsilon_o}\right]} \qquad (1a)$$

where h_p is the thickness of the entire paper, h_c is the height above which the filled section of paper begins, h_T the height at the bottom of the toner layer and h_g is the height of the entire toner-air-paper transfer region (as defined in Fig. 4(a)). The constant ρ is the charge density of the toner, while q_T is the charge on the toner, ε_o is the dielectric of air, ε_c is the dielectric of cellulose, ε_T is the dielectric of the toner and ε_f represents the equivalent dielectric constant of the filled layer of the paper.

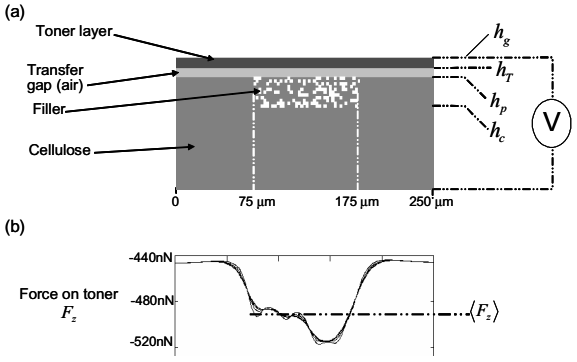

Figure 4. (a) Section of paper showing in three layers from top to bottom: toner, air and paper. The paper is represented as pure cellulose loaded with filler in a small zone near the surface. Fig. 4(b) shows the resulting electrostatic force as a function of the position in the paper section. Multiple toner transfer force lines correspond to the difference in the toner layer thickness ranging from 10 μm to 30 μm.

With the simplest assumption as suggested by experiments on the overall dielectric of paper,[7] ε_f can be expressed in the form,

$$\varepsilon_f = \alpha C + \beta \qquad (1b)$$

where C is the filler concentration and α and β are empirical constants. We fit Eq.(1a) to the simulation data of Fig. 4 using Eq. (1b) with α = 19, β = 1.75 for the case of near-surface filler and α = 18.5, β = 1.9 for the case of filler distributed throughout the bulk.

Surface Filler

Figure 4(b) shows profiles of the z-directional toner transfer force field F_z over the paper with surface fillers at various toner-paper gap distances ($h_g - h_t$) ranging from 10 μm to 30 μm. These profiles were calculated from the continuous model. As can be seen, toner-paper gap did not change toner transfer force profile drastically, however local filler concentrations had more effect on the toner force field profile. We then determined the average transfer force, $\langle F_z \rangle$ shown as broken line in Fig. 4(b), over the area where a given amount of filler is present (Fig 4(a)). We then calculated average transfer force $\langle F_z \rangle$ for various filler concentrations ranging from 0% to 12% and compared them with values calculated using Eq. 1(a), shown as the top curve in Fig. 5. Both the simulation values fit nicely with, the

theoretical curve, showing that the dielectric is essentially a function of the filler concentration. Note that at C =0, the effective dielectric $\varepsilon_{f,}$ is supposed to be equal to $\beta = \varepsilon_c$ (= 3, dielectric of cellulose itself), which will yield <Fz> = - 450. The dielectric value for Ec ranging from 2 ~ 3.[16] however Ef in Eq (1-B), which should be equal to Ec was found to be 1.75 – 1.9. This discrepancy is likely due to the fact that the simple capacitor model of the system is only accurate when the lateral dimension of the system is much larger than the transfer gap thickness. For the lateral system dimensions simulated (100μm), $\varepsilon \approx \beta \approx 2$ is thus only of effective value.

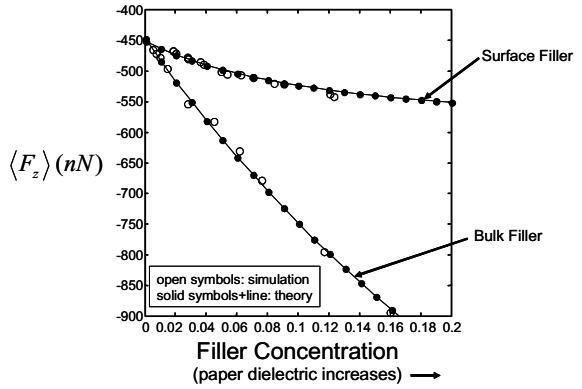

Figure 5. Average toner transfer force vs. filler concentration for fillers distributed near the surface and for fillers distributed in the bulk. The open circles are from numerical simulation of the full electrostatic transfer model. Closed circles are from a theoretical fit to the data assuming a simple capacitor model of the transfer gap, with paper having an effective dielectric.

Bulk Filler

To compare the effect of surface filler vs bulk filler, we then calculated average toner transfer force $<F_z>$ for the bulk filler configuration for the same concentration ranges. Figure 5 shows average toner transfer force $<F_z>$ as a function of filler concentration for two types of paper, one with surface filler and the other with bulk filler configurations. It was no surprise to find that average toner transfer force, $<F_z>$, increased with increasing filler concentration, however it was somewhat a surprise to find that $<F_z>$ for the bulk filler paper was greater than that for the surface filler paper for the same filler concentration. For example, the toner transfer force at approximately 12% filler concentration distributed near the surface, leads to comparable toner transfer force at about 2~3% filler concentration distributed uniformly throughout the bulk. As a result, the bulk filler can cause a much larger variation in toner transfer force than the surface filler. Therefore an optimal design strategy for paper used for electrophotographic printing is to distribute filler uniformly near the surface.

3. Effect of Filler Distribution in the Sheet Plane on Toner Transfer Density

In this section we quantify how in-plane spatial variations in the dielectric at different wavelength (i.e., feature sizes) affect in-plane variations in the corresponding toner transfer force.

Figure 6 (top) illustrates two types of filler distribution with different periodicity. We examine a special case in which filler is distributed within a thin layer near the surface. Also there is no air gap present, implying a "kissing contact" between paper and toner. (The general conclusions of this section are not altered in the presence of air gap.) The periodicity of the filler distributions in the left-hand case occurs at a wavelength $\lambda_{1,}$ while in the right-hand case at a shorter wavelength λ_2. We model periodic variation of the dielectric mathematically as

$$\varepsilon(x) = \varepsilon_u(z) + \delta_q \varepsilon_f [\theta(h_p - z) \cdot \theta(z - h_c)] \sin(2\pi x/\lambda), \quad (2)$$

where $\varepsilon_u(z) = \varepsilon_p$, the average dielectric of the paper for $z < h_c$, and $\varepsilon_u(z) = \varepsilon_t$ the dielectric of toner for $z > h_p$. The function $\theta(x)$ is the unit step function, defined as $\theta(z) = 0$ if $z < 0$ and $\theta(z) = 1$ if $z > 0$. The constant ε_f is the average dielectric of the filled section, while δ_q is considered a small number whose effect is to perturb the total dielectric of paper slightly from the value given by ε_p. The dielectric alternates in magnitude with a sinusoidal wavelength λ. The filler layer is defined between $h_p = 100\mu m$ and $h_c = 50\mu m$, while the entire print gap is $h_g = 110\mu m$. We note that understanding the effects of a simple sinusoidal variation of the dielectric as given by Eq. (2) is useful. This can then be used to predict how any *generalized* dielectric distribution affects toner transfer efficiency. Specifically, the second term of Eq. (2) can be fit to the term of corresponding wavelength in the frequency decomposition of an arbitrary dielectric variation.

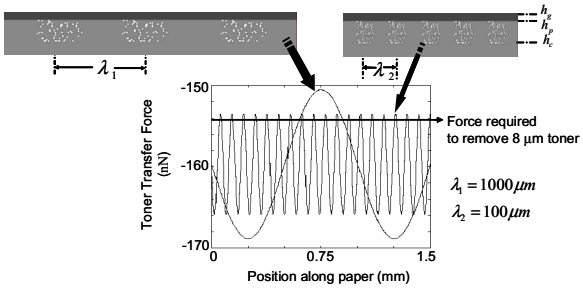

Figure 6. Different length scales of spatial variation of filler lead to different amplitudes of variation in toner transfer force in the transfer gap, due to the dependence of dielectric on filler.

Figure 6 (bottom) shows the toner transfer force corresponding to the dielectric variations at two specific wavelengths, $\lambda_1 = 1000\mu m$ and $\lambda_2 = 100\mu m$. Since toner transfer proceeds from top to bottom, peaks imply a lower transfer force, and troughs a higher force. The horizontal line denotes the minimum force required transferring a typical 8

μm toner.[9] The data demonstrate that the variation in toner transfer force is larger at longer wavelength of dielectric periodicity. The particular wavelengths λ_1 and λ_2 were chosen because they are characteristic of two important length scales of the variation in filler distributions in copy-grade paper.[4] The smaller of the two, λ_2 = 100μm, is close to the smallest scale of variation barely discernable by the human eye at normal reading conditions. The larger, λ_1 = 1000μm, represents a clearly visible scale of variation.

The data in Fig. 6 show that the λ_2 oscillations in dielectric cause the transfer force to just fall short of the threshold for transfer of 8μm toners once every 100 μm (i.e. force rises above horizontal line). Thus, a *minor* reduction of toner transfer (if these were the only types of toners) would occur on length scales barely visible by normal human perception. This would thus be perceived as "uniform". For the λ_1 oscillations in dielectric, the transfer force falls *significantly* short of the threshold of transfer of 8 μm toners once every 1mm, leading to a higher contrast, visible non-uniformity in toner transfer. This is shown in Fig. 7, which plots this transfer force against the wavelength of variation. It is noted that the toner transfer force variation increases drastically with wavelength and approaches a fairly constant value toward λ ~ 1 mm. It is also noted that, above the critical wave length around λ ~ 500 μm, the "peak" toner transfer force (the weakest transfer force) within the variation becomes less than the minimum toner transfer force (-154 nN) for the 8μm particle. These results suggest that a marked variation in paper dielectric on the scale of 500μm or larger contributes significantly to toner transfer force variations, which produce higher contrast in print density variation as a result of missing toner transfer. These results support the findings of Ref. [4].

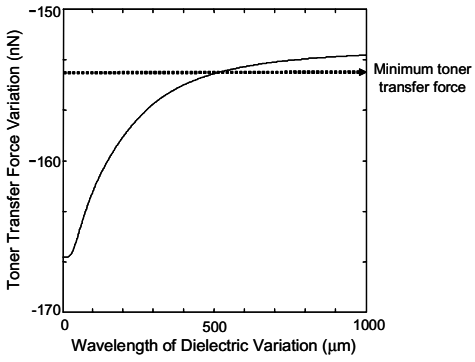

Figure 7. Toner transfer force variation vs. the wavelength of dielectric variation.

4. Effect of Thickness Variation (or Surface Profile) on The Toner Transfer Forces

Another feature that is in the data of Fig 2 is the dependence of toner transfer forces on caliper variations. To understand the source of this effect, we consider the electrostatic field in the transfer gap illustrated by Fig. 1, focussing only on average properties within a given cell "j". Using Eq.(1) and neglecting, for illustrative purpose, the toner (i.e. $h_c = 0$ and $h_T = h_g$, $\rho = 0$), the electric field in the air gap in cell "j" is given by the following simple expression,

$$\langle E_z \rangle_j = \frac{-V}{h_d \left[1 - \left(\frac{\langle \varepsilon_p \rangle - 1}{\langle \varepsilon_p \rangle} \right) \frac{\langle h_p^j \rangle}{h_d} \right]} \tag{3}$$

where h_p^j denotes the thickness of the paper in cell "j" and $\langle \varepsilon_p \rangle$ the average dielectric of paper in the cell. The top paper surface is taken as the reference to measure thickness. The constant h_d is the thickness between the photoreceptor plate and the bottom of the paper. Inspection of this formula shows that even for perfectly uniform paper dielectric constant, there are still variations in the electric transfer in the air gap due to variations in local *thickness* $\langle h_p^j \rangle$. Equation (3) is plotted in Fig. 8 as a function of the paper thickness h_p and local paper dielectric $\langle \varepsilon_p \rangle$. It shows a clear effect of paper thickness on toner transfer forces, particularly as the dielectric of the paper is increased (e.g., more filler added).

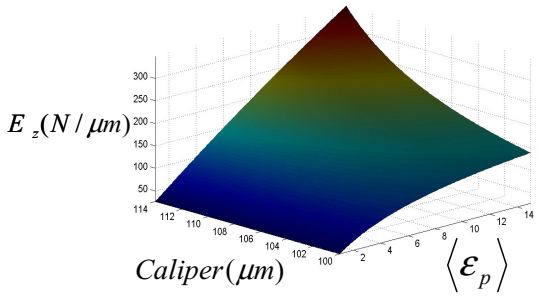

Figure 8. (a) Filled paper cross section. (b) Electrostatic force fields within paper-air transfer gap. Shades of gray represent field strength, with white being the highest field and black the lowest. The force field shows higher values in filler-rich zones of the paper.

Figure 9(a) shows the top surface profile of an unfilled paper, obtained from a digitized micrograph cross section. The bottom surface was assumed to be flat cut of the actual image. The paper was placed in a "virtual" transfer gap and the electric field was calculated. Filler was added uniformly in all pores of the paper at a concentration of 5%. Figure 9(b) shows a surface profile of the same paper as Fig. 9(a), except the filler is added to all pores uniformly at a concentration of 25%. Filler was artificially implanted into the paper this way to simulate the caliper non-uniformity of two sheets with *different* filler contents. Figures 9(c) and (d) show the corresponding toner transfer fields for the cases of Figs. 9(a) and (b), respectively. The field plots show that higher filler

content clearly produces a larger *offset* in toner transfer force. This is expected from the discussion on the general effect of filler. However, in both figures there tends to be an inverse correlation of the electrostatic field with the caliper variations, at longer length scales around 500 μm to 1 mm. These scales of variation provide an additional mechanism for the scales of print density variation observed in the data of Ref. [4].

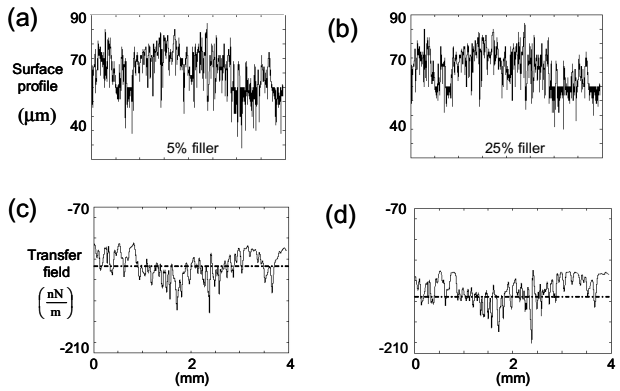

Figure 9. Figures 9(a) and (b) show caliper profiles of two paper samples, obtained from a micrograph. While nearly identical in profile, the two paper samples contain two distinct levels of filler distributed in the same manner throughout the bulk (and not visible in the Figs.9(a) and (b)). Figure 9(c) and (d) show the toner transfer field corresponding to the profile of Fig. 9(a) and (b) within an electrophotographic transfer gap. The paper in Fig. 9(b) produces a larger electrostatic field owing to its higher overall filler content. In both cases, however, the long scale modulations of the transfer reflected closely the caliper variations.

Equation 3 shows that non-uniform caliper variations and material dielectric can be conveniently "packaged" into an effective or equivalent "dielectric" of the paper. Thus toner transfer force variations can be generally attributed to effective dielectric variations, as caused by material non-uniformity and caliper variations.

Conclusion

In this report we examined quantitatively how filler distributions in the in-plane and z-direction of paper as well as caliper variations affect toner transfer.

We found that, at the same filler content, the toner transfer force is greater for the uniform filler distribution throughout the thickness than for the filler distribution only in a thin surface layer. We also found that the in-plane dielectric variations significantly contribute to toner transfer force variations on the scale above 500 μm. In addition, we found that the higher the filler content, the greater the toner transfer force variation caused by caliper non-uniformity. It is expected that other factors such as moisture and salts will have similar effects through their own contribution to paper dielectric. These factors will be examined in upcoming reports.

References

1. J. Johnson, *"Principles of Non-impact Printing",* Palatino Press, Irvine, USA (1992).
2. R.M. Schaffert, "*Electrophotography*", Focal Press, New York (1975).
3. R.B. Comizzoli, G.S. Lozier and D.A. Ross, "*Electrophotography –A Review*", RCA Review, 33, 406 (1972).
4. N. Provatas, A. Cassidy, and M. Inoue, IS&T's NIP 18, San Diego, 2002, pg. 770
5. J. Aspler, Miscellaneous Report 429, Pulp and Paper Research Institute of Canada (2000).
6. N. Provatas and T. Uesaka, JPPS, 29(10), 332 (2003).
7. S. Simula, S. Ikalainen , K. Niskanen, T. Varpula, H. Seppa and A. Paukku, J. Imag. Sci. and Tech. 43(5), 472 (1999).
8. M.-K. Tse, D.J. Forrest and F.Y. Wong, IS&T's NIP 15, 1999, pg. 486
9. R.J. Trepanier, Tappi J., 72(12), 153 (1989).
10. M. O'Neill and B. Jordan, JPPS, 26(4), 131 (2000).
11. P.M. Chaikin and T.C. Lubensky, "*Principles of Condensed Matter Physics*", Cambridge University Press, Cambridge, UK (1995).
12. L.D. Landau and E.M. Lifshitz, "*Electrodynamics of Continuous Media*, 2 nd *Edition",* Butterworth-Heinemann, Woburn, MA. (1960).
13. C.C. Yang, G. Hartman, IEEE Transactions on Electron Devices, 23(3), 308 (1976).
14. J.Q. Feng and D.A. Hays, J. Imag. Sci. and Tech., 44(1), 19 (2000).
15. W.H. Press, S.A. Teukolsky, W.T. Vetterling and B.P. Flannery, "*Numerical Recipes in Fortran 2nd Edition*", Cambridge University, Cambridge, UK, (1992).
16. C. R. Calkins, Tappi Journal 33(6), 278 (1950)

Biography

Mitsuo Inoue received a B.Sc. (1965) and a M.Sc. (1967) in Colloid and Surface Chemistry from Tokyo Metropolitan University. Since he joined the Pulp and Paper Research Institute of Canada (Paprican), his research has been dealing with the aspect of wetting and adhesion in paper products. He is currently involved with surface modification of digital non-impact printing papers. He is a member of ACS, Tappi and IS&T.